

Advanced photovoltaic inverter functionality verification using 500kW Power Hardware-in-Loop (PHIL) complete system laboratory testing

Barry A. Mather, *Member IEEE*, Matthew A. Kromer, and Leo Casey, *Member IEEE*

Abstract-- With the increasing penetration of distribution connected photovoltaic (PV) systems, more and more PV developers and utilities are interested in easing future PV interconnection concerns by mitigating some of the impacts of PV integration using advanced PV inverter controls and functions. This paper describes the testing of a 500kW PV inverter using Power Hardware-in-Loop (PHIL) testing techniques. The test setup is described and the results from testing the inverter in advanced functionality modes, not commonly used in currently interconnected PV systems, are presented. PV inverter operation under PHIL evaluation that emulated both the DC PV array connection and the AC distribution level grid connection are shown for constant power factor (PF) and constant reactive power (VAr) control modes. The evaluation of these modes was completed under varying degrees of modeled PV variability.

Index Terms— Power hardware-in-loop (PHIL), high power photovoltaic (PV) inverter testing, advanced PV inverter functionality, power factor control, reactive power control

I. INTRODUCTION

The continued high rate of deployed distribution system connected photovoltaic (PV) systems, particularly megawatt-scale ground and roof mounted systems, has led to interest by PV developers and utilities in the impact of PV systems interconnected on the distribution system. Additionally, once distribution system level impacts have been determined, the mitigation of negative impacts is of foremost interest to the PV developers and distribution utilities in order to accommodate the interconnection of increasing penetration levels of PV without expensive equipment upgrades or reduced distribution system performance. The Southern California Edison (SCE) High-Penetration PV Integration Project [1], led by the National Renewable Energy Laboratory (NREL), is in the

second year of a five year project that aims to identify and quantify the impacts of distribution system-connected PV systems, and to demonstrate potential PV impact mitigation methods. The experiment described in this paper was completed under the auspices of the SCE High-Penetration PV Integration Project. The team that completed the experiment included SCE High-Penetration PV Integration Project team members and the Center for Advanced Power Systems (CAPS) at Florida State University (FSU) where the laboratory testing was completed.

Many different concepts for PV impact mitigation on the distribution system have been proposed. The SCE High-Penetration PV Integration Project has focused on PV impact mitigation via advanced control functionality integrated into the PV inverter. The reason this approach was adopted is that PV mitigation at the point of grid interconnection (often at or very near a PV systems inverter(s)) is likely the most effective and realistic mitigation approach. Additionally, the PV inverter is a likely candidate for providing mitigation functionality, as it can provide some forms of potential PV mitigation, such as VAr support functions, with a low incremental cost. A description of potential PV mitigation VAr support functions is given in [2]. Also, an effort is underway to standardize the utility communications interface to inverters and other equipment providing PV mitigation services [3].

This paper describes the results of a testing effort that was designed to examine both the ability of a PV inverter to provide advanced functions, designed to mitigate PV impact issues on the distribution system, and to quantify the efficacy of the implemented advanced PV inverter functions on their ability to reduce the distribution system level impacts of interconnected PV systems. While the testing completed addressed both of these issues, this paper focuses only on the ability of a PV inverter to implement two advanced functionality PV inverter functions that show potential usefulness in mitigating the impacts of PV interconnection. The two functions tested were the operation of the PV inverter under constant power factor (PF) control and under constant reactive power (VAr) control. While these two modes of operation are relatively basic they are considered “advanced functions” as these modes of operation are generally

Barry A. Mather is with the Distributed Energy Systems Integration (DESI) Group at the National Renewable Energy Laboratory (NREL), Golden, CO 80401 USA (e-mail: barry.mather@nrel.gov). Matthew A. Kromer and Leo Casey are with Satcon Technology Corporation, Boston, MA 02210 USA (e-mail: matthew.kromer@satcon.com, leo.casey@satcon.com).

considered to be outside the modes of operation typically allowed by the IEEE 1547 distributed resource interconnection standard [4].

Power Hardware-in-Loop (PHIL) testing of the PV inverter was selected for this evaluation in order to analyze the operation of the PV inverter under “near” real world interconnection conditions. All reasonable efforts were taken to make the PHIL experiment as applicable to the actual deployment of an advanced functionality PV inverter in SCE’s distribution system as planned in the out years of the SCE High-Penetration PV Integration Project.

Section II of this paper gives a brief description of the PHIL experiment and presents the baseline operation of PV inverter without advanced functionality enabled. Sections III and IV present the results of the completed PHIL testing for the PV inverter operating with constant PF and constant VAR control modes enabled respectively. Section V concludes the paper.

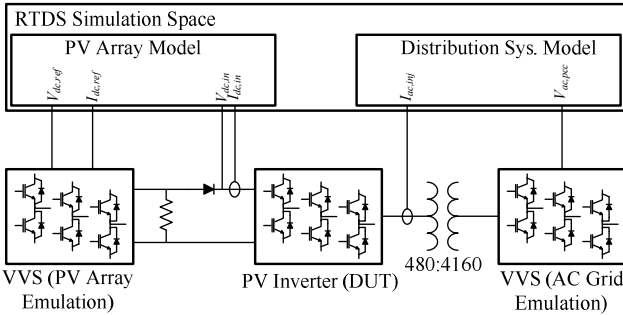


Fig. 1. Simplified diagram of the PHIL experimental setup showing the AC and DC interconnection of power electronic based Variable Voltage Sources (VVS) that are controlled through the Real-Time Digital Simulator (RTDS) system to emulate both the DC PV array and AC grid equipment interconnections.

II. POWER HARDWARE-IN-LOOP (PHIL) EXPERIMENTAL SETUP DESCRIPTION

A brief description of the PHIL experimental setup is given in this section. A more detailed description of the experiment setup and a discussion of the testing completed is given in [5]. As this PHIL experiment aimed to simulate real world operation the experiment runs in real-time and each test run completed was 16 minutes in simulation duration.

A. PHIL Experimental Setup

Fig. 1 shows a simplified diagram of the various components used to complete the PHIL testing. The PV inverter is shown in the center of the diagram. The inverter used in the experiment was a Satcon 500kW Power Gate Plus with a native AC output voltage of 200V_{ac} nominal. The inverter interfaces to two Variable Voltage Sources (VVS’s). These VVS’s consist of high power electronic modules similar to the PV inverter under test. The VVS used for PV array emulation (the “DC VVS”) is configured to output DC power to the PV inverter’s DC input terminals. A small load was connected in parallel to the PV inverter under test to provide a minimum load should the PV inverter “trip” off-line due to internal protection functions. This load ensured that the voltage of the PV array emulating VVS would not rise too high during a PV

inverter trip and damage the PV inverter. A diode was also installed in the series path of PV array connection so that the PV inverter could not backfeed power to the VVS under any circumstances. Again, this was done to protect the VVS being used for PV array emulation from high voltage transients.

A second VVS (the “AC VVS”) was configured to provide the emulation of the PV inverters interconnection to the distribution system (AC grid). In this case a transformer (480V:4160V) was used to interface the PV inverter’s AC output to the VVS. As the PV inverter’s AC operating voltage was nominally 200V_{ac} the VVS was operated at a lower voltage on the primary to match the secondary transformer voltage of 200V_{ac} nominal.

The remaining critical component to the PHIL testing was the use of two models in the Real-Time Digital Simulator (RTDS). This functionality is shown by the connection of measured signals within the system, namely the PV inverter’s DC input voltage and current and the three-phase output current of the PV inverter, to functional boxes in the RTDS Simulation Space. These signals were processed through models of both the PV array model and the interconnected distribution system model to produce operational references (or set-points) that were used to control the two VVS’s.

B. PV Array Emulation

Fig. 2 shows the two relative PV array power output profiles used to drive the PV array model shown in Fig. 1. Two profiles were generated based on measured 1 second PV irradiance profiles from NREL’s Measurement and Instrumentation Data Center (MIDC) [6]. A 5 second moving average was applied to the data in order to approximate the spatial variability reduction of a 500kW PV array as compared to the single point irradiance measurement. Additional details on the implementation of the PV array model realized in the RTDS are given in [5].

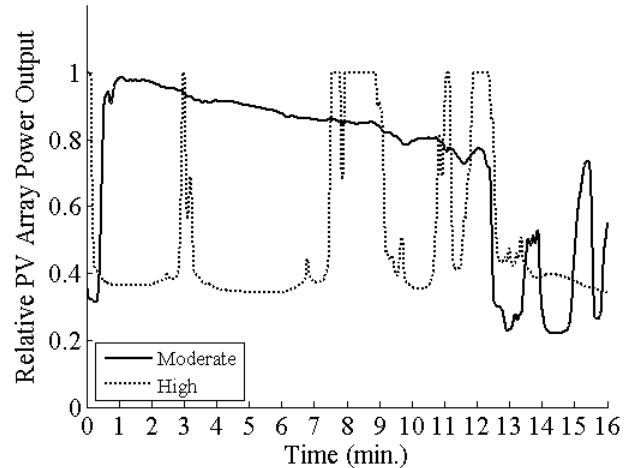
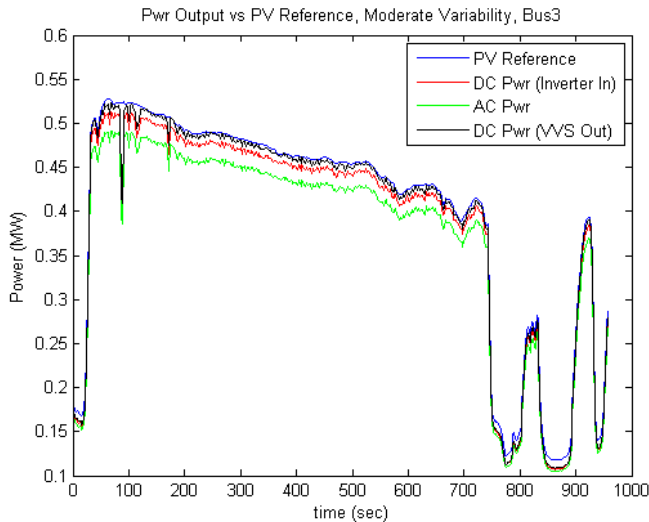


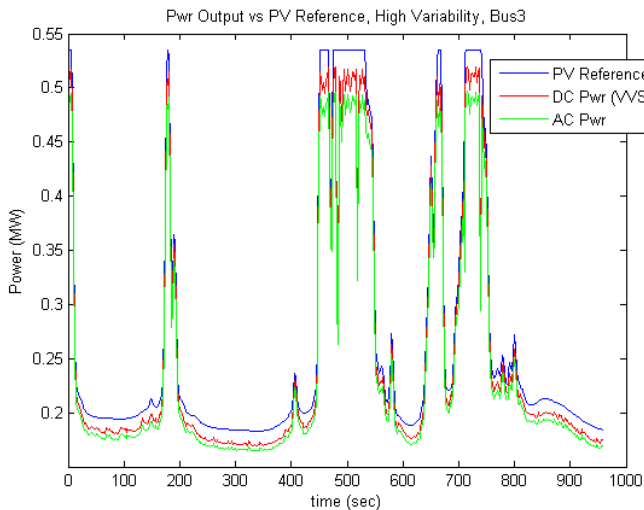
Fig. 2. Relative PV array power output profiles used during PHIL testing based on normalized moderate and high PV array irradiance profiles.

C. AC Grid Interconnection Emulation

A simplified RSCAD model of the Fontana, CA High-Penetration PV Study Circuit, described in [2], was developed for this experiment. The distribution system model included time varying loads and emulated controllers for the multiple switched capacitors (for voltage regulation) located on the circuit. During PHIL test runs, the three-phase output current of the PV inverter was sampled at a high frequency. The currents were added to the distribution system model and the point of PV inverter interconnection three-phase voltage was determined. This three-phase voltage was used as the reference (with the appropriate scaling) as the voltage reference for the AC VVS. In this manner, the effective impedance at the PV inverter's point of interconnection as modeled in the Fontana, CA Study Circuit was varied as



(a) DC and AC power balance through the PV inverter over the moderate irradiance variability test case



(b) DC and AC power balance through the PV inverter over the high irradiance variability test case

Fig. 3. Plots of the PV Reference (power available from the emulated PV array), DC Power (power delivered from the DC VVS), DC Power Input (power input in the DC connections of the inverter under test), and AC Power (power output from the PV inverter under test) for both the moderate and highly variable PV array irradiance profiles (16minute / 960 second test runs)

conditions on the distribution circuit and the available PV array power changed during the PHIL simulation.

D. Baseline Operation of the PV Inverter without Advanced PV Inverter Functionality

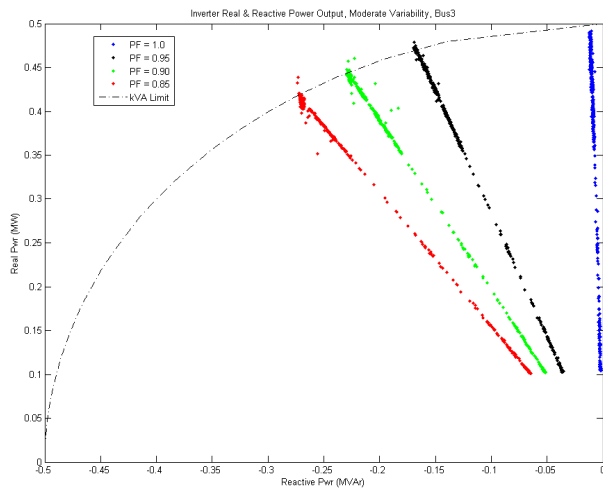
Prior to the evaluation of advanced PV inverter functions the general PHIL implementation, including both the PV array and distribution system interconnection emulation, was extensively tested to insure that the PHIL simulation was sufficiently stable and produced the expected operational characteristics. Fig. 3(a) shows the DC and AC power balance through the PV inverter under test. The figure shows the PV power reference profile, the DC input power to the PV inverter, the AC output power of the PV inverter and the DC power output from the DC VVS for the moderate PV variability case. Inspection of the plot shows that the DC power output of the VVS tracks the PV reference as the PV array power varies. The DC power input to the inverter is slightly lower than the available power from the DC VVS due to the small resistive load connected in parallel with the inverter input for equipment protection reasons. Additionally, the AC output power of the PV inverter lower than the DC input power to the inverter due to non-unity inverter efficiency. Fig. 3(b) shows a similar set of curves to those shown in Fig. 3(a), but corresponds to the high variability case. The data in the high variability shows similar characteristics to those in the moderate case, with the exception that DC VSS tracking is not perfect during periods of very high PV array output (due to PV inverter DC input saturation).

III. PV INVERTER OPERATION IN POWER FACTOR CONTROL MODE

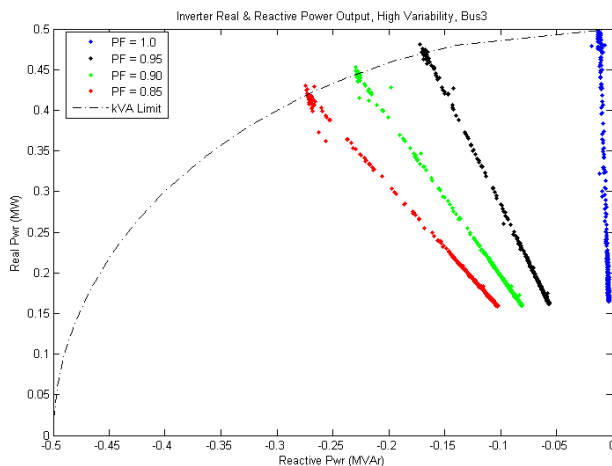
The PV inverter was operated in constant power factor control mode at four separate PF settings, 1.0, 0.95, 0.9 and 0.85. All non-unity PF settings were inductive (absorbing VARs) so that the voltage rise seen at the inverters point of interconnection due to real power injection (caused by a reduction in the I^2R losses incurred to deliver power to loads at point on or near the PV inverter injecting real power) was counteracted by a voltage drop caused by increased losses due to the increased reactive power flow. The PV inverter controlled the PF so that it remained constant regardless of how much real power was injected into the modeled distribution circuit.

Fig. 4(a) shows a time-independent X-Y plot of the PV inverters real and reactive power salient operating points for the various constant PF settings and for a PHIL simulation run using the moderate PV array power variability profile. The straight lines of varying slope show the expected operation of the PV inverter under constant PF operation. The curved dashed line on the plot shows the rated MVA limit of the PV inverter tested. Fig. 4(b) presented the same information as Fig. 4(a) but for the high PV array power variability profile. Larger intermittent PF measurement excursions from the expected constant PF operation of the PV inverter are seen particularly at higher real power operating points. Fig. 5(a) and 5(b) show the same information as plotted in Fig. 4(a) and

4(b) but are plotted as a function of PHIL simulation time. Fig 5(a) presents the PV inverter operating power factor for the PHIL experiment utilizing the moderate variability PV array power profile and 5(b) presents the same but for the high variability PV array power profile. These figures also clearly show that the PV inverter had to curtail some production of real power during periods of high PV array irradiance for non-unity PF settings. This is due to the finite current limit and thermal management limit of the PV inverter being tested. VARs can be supplied to or absorbed from the distribution system but at a cost of either reduced real power production at certain times or increased PV inverter power processing capability.

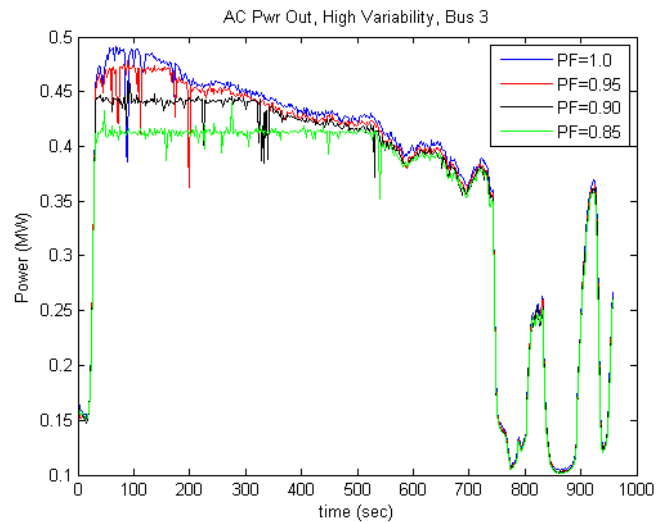


(a) X-Y plot of the real and reactive power during 16 minute real-time PHIL simulations for constant PF control mode set-points of 1.0, 0.95, 0.90, and 0.85 for the moderate PV array power variability case

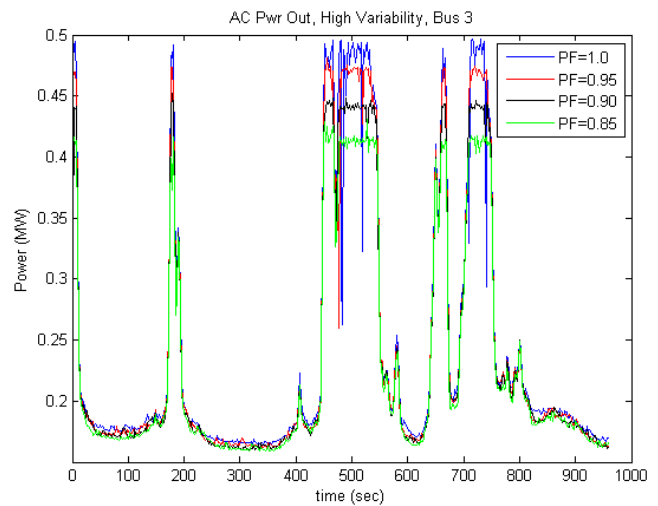


(b) X-Y plot of the real and reactive power during 16 minute real-time PHIL simulations for constant PF control mode set-points of 1.0, 0.95, 0.90, and 0.85 for the high PV array power variability case

Fig. 4. Plots of the salient operating points (real and reactive power) of the PV inverter under test for moderate and high variability PV array power profiles with the constant PF mode enabled



(a) PV inverter real power output for PF set-points of 1.0, 0.95, 0.9, and 0.85 for the moderate PV array power output variability case



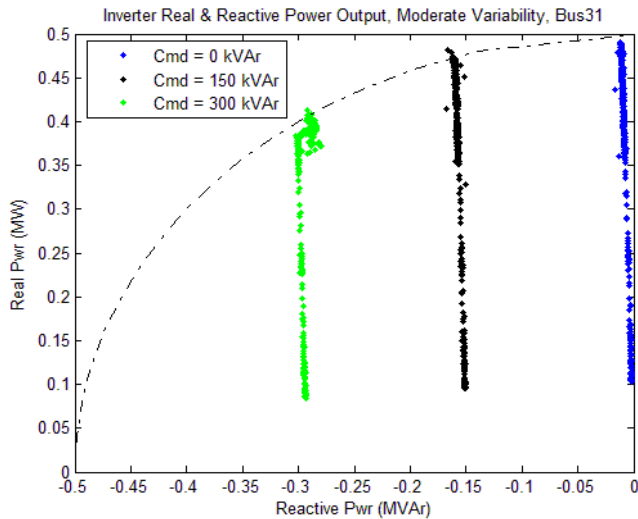
(b) PV inverter real power output for PF set-points of 1.0, 0.95, 0.9, and 0.85 for the high PV array power output variability case

Fig. 5. Plots of the PV inverter real power output, showing real power curtailment due to the PV inverters power processing limit (VA), during PHIL simulation runs for moderate and high PV array power variability

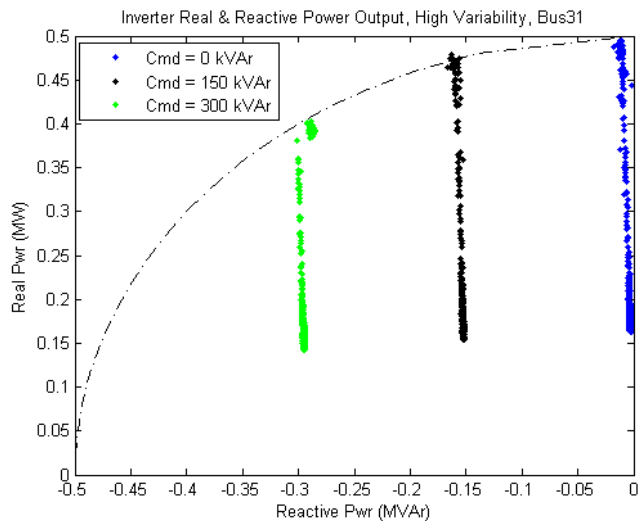
IV. PV INVERTER OPERATION IN CONSTANT REACTIVE POWER CONTROL MODE

The PV inverter was also tested for its ability to provide a constant amount of reactive power mitigation support for the distribution grid regardless of the amount of real power the PV inverter was processing. This mode of operation would emulate the way that some distribution utilities currently maintain voltage regulation along their distribution circuits by using switched capacitors (supplying VARs to increase the voltage/ reduce voltage losses). The PV inverter was tested under the condition that VARs were being absorbed at the point of the PV inverter interconnection. Identical to the constant PF operating test described above, VARs were absorbed at the point of the PV inverter interconnection to effectively lower the voltage at that point (or reduce that amount of voltage rise seen at that point). However, in this case the amount of

reactive power absorbed was not a function of how much real power the PV inverter supplied to the distribution circuit. The amount of reactive power requested to be absorbed by the PV inverter was kept constant during the entire PHIL simulation run. Figs. 6(a) and 6(b) show the time-independent plot of the PV inverters salient operating real and reactive power during the 16 minute PHIL simulation test runs with constant reactive power settings of 0, 150 and 300kVAr. The straight vertical lines indicate that the reactive power absorbed by the PV inverter is constant regardless of the real power operating level. Small deviations in the amount of reactive power absorbed compared to the requested amount are seen near the operating kVA limit of the PV inverter and are particularly visible for the case when 300kVAr was requested from the PV



(a) X-Y plot of the real and reactive power during 16 minute real-time PHIL simulations for constant reactive power control mode set-points of 0, 150 and 300kVAr for the moderate PV array power variability case



(a) X-Y plot of the real and reactive power during 16 minute real-time PHIL simulations for constant reactive power control mode set-points of 0, 150 and 300kVAr for the high PV array power variability case

Fig. 6. Plots of the salient operating points (real and reactive power) of the PV inverter under test for moderate and high variability PV array power profiles with the constant reactive power mode enabled

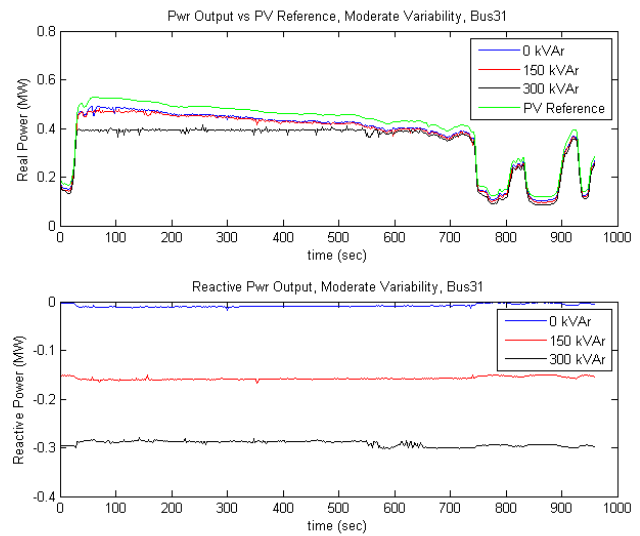


Fig. 7. Plots of the PV inverter real power output (top) and reactive power output (bottom) during PHIL simulation runs for moderate and high PV array power variability

inverter. Such deviations are small and the ability of the PV inverter to absorb a nearly constant amount reactive power during the PHIL experiment duration is confirmed by the collected data.

Fig. 7 shows the real power provided to the distribution circuit and the reactive power absorbed from the distribution circuit over the period of the simulation for each constant reactive power set-point. Again, the real power produced is limited during periods of high PV array irradiance particularly for the case when 300kVAr is constantly absorbed by the PV inverter. This is again due to the physical capacity constraints (current and thermal) of the PV inverter and is not due to the specific control implemented in the PV inverter. The reactive power plot shows that the amount of reactive power absorbed is nearly constant during the entire test run, providing evidence that such operation is feasible.

V. CONCLUSIONS

This paper presents the analysis of data collected during a rigorous PHIL experiment testing the ability of a PV inverter to provide advanced volt/VAr based services for the mitigation of the distribution system level impacts of PV system integration. The PV inverters ability to operate under both a constant PF and constant reactive power set-point mode were evaluated. Furthermore, the ability for the PV inverter to provide these functionalities was tested over two different PV array power variability profiles (moderate and high variability). In all cases the PV inverter performed these functions well. It was also shown that real power curtailment does occur, due to the finite current and thermal limits of the PV inverter, during periods of high PV array irradiance and is particularly noticeable when large amounts of reactive power (a low PF or high kVAr set-point) are requested of the PV inverter. The balance between the loss of captured PV energy and the reduction of the distribution system level impacts

encountered by high-penetration PV integration need to be carefully considered and are a topic for further research.

VI. ACKNOWLEDGMENT

This work was supported by the U.S. Department of Energy, under Contract No. DOE-AC36-08-GO28308 with the National Renewable Energy Laboratory, and the California Public Utility Commission under a California Solar Initiative (CSI) Research, Development, Demonstration, and Deployment (RD&D) Program grant.

VII. REFERENCES

- [1] DOE SunShot Initiative High Penetration Solar Portal – *NREL: Analysis of High Penetration Levels of Photovoltaics Into the Distribution Grid in California – SCE High-Penetration PV Integration Project*, online resource: https://solarhighpen.energy.gov/project/nrel_analysis_of_high_penetration_levels_of_photovoltaic_into_the_distribution_grid_in_california, accessed Oct., 2012.
- [2] B. Mather, B. Kroposki, R. Neal, F. Katiraei, A. Yazdani, J. R. Aguero, T. E. Hoff, B. L. Norris, A. Parkins, R. Seguin, C. Schauder, “*Southern California Edison High-Penetration Photovoltaic Project – Year 1 Report*,” NREL Technical Report TP5500-50875, 2011.
- [3] B. Seal, Presentation – *Smart Inverter Communication Initiative – Project Overview and Status*, online resource: <http://www.4thintegrationconference.com/downloads/Inverter%20Seal.pdf>, accessed Oct. 2012.
- [4] IEEE 1547 *IEEE Standard for Interconnecting Distributed Resources with Electric Power Systems*, IEEE Standard, 2003.

- [5] J. Langston, K. Schoder, M. Steurer, O. Faruque, J. Hauer, F. Bogdan, R. Bravo, B. Mather, F. Katiraei, “*Power Hardware-in-the-Loop Testing of a 500kW Photovoltaic Array Inverter*,” in proc. of IEEE Ind. Elect. Conf., Oct., 2012
- [6] NREL Measurement and Instrumentation Data Center (MIDC), online resource: <http://midc.nrel.gov>, accessed Oct., 2012.

VIII. BIOGRAPHY

Barry A. Mather (S’2003, M’2010) received the B.S. and M.S. degrees in electrical engineering from the University of Wyoming, Laramie, WY, in 2001 and 2004 respectively and the Ph.D. degree also in electrical engineering from the University of Colorado, Boulder, CO, in 2010. In March 2010 he joined the Distributed Energy Systems Integration (DESI) Group at the National Renewable Energy Laboratory (NREL), Golden, CO, where he is currently researching distributed photovoltaic energy system integration issues. His research interests include the analysis and mitigation of high-penetration PV integration into the distribution system as well as advanced power electronic applications in renewable energy systems.

Matthew A. Kromer received BS and MS degrees in electrical engineering from Brown University in 1999 and 2000, respectively, and an MS in Technology and Policy from the Massachusetts Institute of Technology (MIT) in 2007. He joined Satcon, an advanced electronics company focused on Grid Support and Alternative Energy, in 2011 as the R&D Program Manager, where he is responsible for managing Satcon’s advanced inverter development activities. Prior to joining Satcon, Matthew worked at TIAX, a clean energy technology firm, as a technical consultant and analyst. His research interests include integration of renewables and energy storage with the electric grid.

Leo Casey received the B.E. degree from the University of Auckland, N.Z. in 1980 and the M.S. and Sc.D. degrees in electrical engineering from the Massachusetts Institute of Technology in 1984 and 1988 respectively. He joined Satcon in 2000 as the Chief Technology Officer, Vice President of Technology and Chief Engineer. Prior to joining Satcon Leo worked at International Totalizing Systems and Philips Electronics.